doi:10.1038/nature11902

1 Materials and Methods

1.1 Qubit fabrication

Josephson junctions and dipole antennas are fabricated on high-purity single-crystal sapphire in one single fabrication step by electron-beam lithography followed by aluminum double-angle electron-beam evaporation. The two evaporations deposit thin aluminium films with a thickness of 20 nm and 60 nm respectively. These layers are separated by an AlOx barrier grown by thermal oxidation for 720 seconds in 2000 Pa static pressure of a gaseous mixture of 85% argon and 15% oxygen.

1.2 Measurement setup

The state of the qubit is probed by measuring the qubit-state dependent cavity transmission using heterodyne detection. Fig. 1 is a block diagram of the measurement setup. Microwave signals for control and measurement transmit through a coax cable with a 20 dB attenuator at 4 K and a 20 dB directional coupler followed by a 10 dB attenuator at 25 mK. The cavity transmission at the output goes through two cryogenic isolators at 25 mK followed by a HEMT amplifier with a noise temperature of 5 K at the 4 K stage. At room temperature, the transmission signal from the cavity is further amplified by two low-noise room temperature amplifiers and is mixed down to a 20 MHz signal which is digitized using a 1 GS analog to digital converter.

2 Full system Hamiltonian

The two cavities, one qubit system, can be described by the Hamiltonian

$$\begin{aligned}\frac{H}{\hbar} = \; & \omega_c a^\dagger a + \omega_m a_m^\dagger a_m + \omega_q b^\dagger b \\ & - \frac{K}{2} a^\dagger a^\dagger a a - \frac{K_m}{2} a_m^\dagger a_m^\dagger a_m a_m - \frac{K_q}{2} b^\dagger b^\dagger b b \\ & - \chi a^\dagger a \; b^\dagger b - \chi_{qm} a_m^\dagger a_m \; b^\dagger b - \chi_{cm} a^\dagger a \; a_m^\dagger a_m\end{aligned} \tag{1}$$

in the strong dispersive limit of circuit QED. Where $a/a^\dagger$, $a_m/a_m^\dagger$, $b/b^\dagger$ the raising/lowering operators for the storage cavity, the measurement cavity and the qubit. The Hamiltonian is calculated by treating the system as three coupled harmonic oscillators and introducing the cosine term in the Josephson relation, using the $\phi^4 \sim (b + b^\dagger)^4$ term in the Taylor expansion, as a perturbation [1]. Higher order terms ($\sim \phi^6$) are more than a factor of 1000 smaller for the parameters of this experiment and can be safely neglected. The Hamiltonian in Eqn.1 of the main text can be recovered from the above Hamiltonian by neglecting all but the lowest two levels of the qubit ($b^\dagger b^\dagger b b = 0$) and replacing $b^\dagger b$ with $\frac{1}{2}(1 + \sigma_z)$. Furthermore all terms $\sim a_m^\dagger a_m$ are zero as the readout resonator always stays in the ground state during the Kerr evolution.

The first three terms in the above Hamiltonian describe each mode as a harmonic oscillator with ω_c the resonance frequency for the storage cavity, ω_m the resonance frequency for the measurement cavity and ω_q the ground to first excited state transition frequency for the qubit. The next three terms describe the anharmonicity of each mode, the anharmoncity of the storage resonator K, the anharmonicity of the measurement cavity K_m and the anharmonicity of the qubit K_q. The last three terms describe the state dependent shifts of each mode due to the state of the other two.

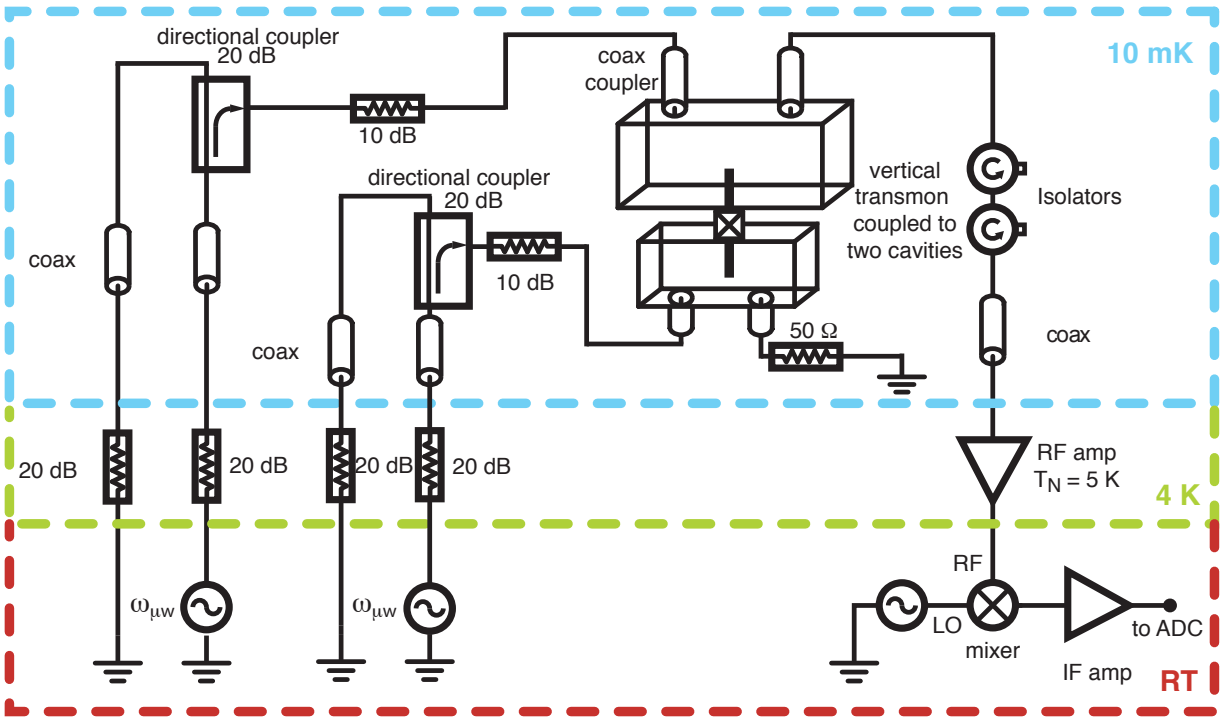

Figure 1: **Block diagram of the measurement setup.**

This means that the transition frequency of a resonator not only depends on the state of the qubit but also on the state of the other cavity. In our system all of these state dependent shifts are much bigger then any decay rate. The state dependent shift of the storage cavity to the qubit is χ, of the measurement cavity to the qubit is χ_{qm} and of the storage cavity to the readout cavity χ_{cm}. The values of all parameters determined by spectroscopy and a comparison to the theory values obtained using finite-element calculations for the actual geometry, combined with "Black-Box" circuit quantization [1] are given in Table 1.

Table 1: Comparison of the experimentally obtained and predicted values for the frequency and anharmonicity of each mode as well as the state dependent shifts between the modes.

	Exp. (MHz)	Th. (MHz)	deviation (%)
$\omega_q/2\pi$	7850.3	7890	< 1
$\omega_c/2\pi$	9274.7	9372	1
$\omega_m/2\pi$	8256.4	8336	1
$K_q/2\pi$	73.4	72	2
$K/2\pi$	0.325	0.25	30
$K_m/2\pi$	3.8	3.7	3
$\chi/2\pi$	9.4	8.2	15
$\chi_{qm}/2\pi$	29.5	29.5	< 1
$\chi_{cm}/2\pi$	2.45	2.1	16

3 Photon number state selective pulses

In order to measure the state of the storage cavity, we must project the cavity onto a photon number (Fock) state. From Eqn. 1, we can see that the qubit transition frequency is dependent on the photon number state of the resonator. As long as the frequency shift, χ, is much larger than spectral width σ of the interrogation pulse, a photon number state selective pulse X_π^m can be performed. In this experiment, $\chi/2\pi = 9.4$ MHz and $\sigma/2\pi = 2.6$ MHz, making a pulse selectivity of $1 - e^{\frac{-\chi^2}{2\sigma^2}} > 0.99$. This is essentially a CNOT [2] operation, with the qubit as the target, conditioned on the photon number in the cavity. A similar scheme to reconstruct the state of a cavity or phonon mode was discussed

in the context of cavity QED and ion traps [3, 4]. This process can be described by

$$|\Psi_{cavity}\rangle \otimes |\Psi_{qubit}\rangle = \sum_{n=0}^{\infty} c_n |n\rangle \otimes |g\rangle \xrightarrow{X_\pi^m} \sum_{\substack{n=0 \\ n\neq m}}^{\infty} c_n |n\rangle \otimes |g\rangle + c_m |m\rangle \otimes |e\rangle . \tag{2}$$

Where the state of the cavity is described as a sum over the Fock states $|n\rangle$ with c_n the complex amplitude. This procedure entangles the qubit and cavity thus a measurement of the qubit state will project the cavity onto the m^{th} photon fock state. The probability of finding the qubit in the excited state is then given by $p_m = c_m^2$ which is exactly the probability of finding the cavity in the state $|m\rangle$.

4 Qubit state readout and Cross Kerr dependence

The state dependent shift between the two cavities, or Cross-Kerr, enables us to readout whether one cavity is in the ground state or not by probing the other cavity exactly like reading out the qubit state. This also means that the qubit cannot be readout independently of the state of the storage cavity so both, qubit and storage cavity, will contribute to the readout voltage. In the experiments we are using the Jaynes Cummings readout [5]. The readout voltage in an experiment measuring Q_m for the state

$$\Psi = c_m |m\rangle \otimes |e\rangle + \sum_{\substack{n=0 \\ n\neq m}}^{\infty} c_n |n\rangle \otimes |g\rangle \tag{3}$$

is given by

$$V_{exp} = p_m V_{e,m} + \sum_{\substack{n=0 \\ n\neq m}}^{\infty} p_n V_{g,n}. \tag{4}$$

with $p_n = c_n^2$ the probability of finding the n-photon Fock state, $V_{g,n}(V_{e,n})$ the readout voltage for the ground(excited) state of the qubit with the resonator in the n-photon Fock state. To remove this effect in our measurements, e.g. determining whether the qubit was excited by a photon number state selective π pulse, we always perform a control experiment without a photon number selective π pulse applied to the qubit. The readout voltage in this control experiment is given by

$$V_{control} = \sum_{n=0}^{\infty} p_n V_{g,n}. \tag{5}$$

Subtracting the two measured voltages from another removes the effect of the resonator excitation

$$V_{exp} - V_{control} = p_m(V_{e,m} - V_{g,m}) \tag{6}$$

This gives us an effective voltage ranging from 0 for the ground state of the qubit to $V_{e,m} - V_{g,m}$ for the excited state of the qubit. This procedure was applied to measure the photon number probabilities for displacing the ground state and all $Q_n(\alpha)$ in the main text. Fig. 2 shows a line cut from $\alpha = 0$ to 4 of the measured Q_0, Q_1, Q_4 for the ground state before subtraction of the control experiment which is also shown in the figure. Subtracting the background experiment from the measured Fock state probabilities leads to the data shown in Fig.3b. This figure shows furthermore that our readout is linear, which means that $V_{g,m} - V_{e,m} = V_{g,0} - V_{e,0}$, as the fit to data is given by a simple Poisson distribution without adjusting for any amplitude correction. This means, that our readout voltage for measuring Q_m is given by

$$V_{exp} - V_{control} = p_m(V_{e,0} - V_{g,0}) \tag{7}$$

with $V_{g,0} < V_{e,0}$ assuming the qubit is initially in the ground state (see section 7).

5 Determining the cavity anharmonicity

The cavity anharmonicity is measured by spectroscopy using a 50 μs pulse to excite the cavity. The cavity excitation is measured by mapping the population left in the ground state to the qubit using a photon number state selective π pulse. The π pulse on the qubit will be successfull only when the cavity is in the ground state after the spectroscopy pulse. Spectroscopy on the cavity for a varying spectroscopy power is shown in Fig.3a. For the lowest power the cavity is only excited on the $|0\rangle \rightarrow |1\rangle$ transition at a frequency of 9.2747 GHz. As the power is increased different transitions appear in the spectroscopy. These transitions are multi-photon transitions from $|0\rangle$ to $|n\rangle$ with $n = 2, 3$ which means the separation between the peaks is given by $0.5\,K/2\pi = 163$ kHz, the Kerr nonlinearity of the cavity. The data were fit using a sum of Lorentzian peaks.

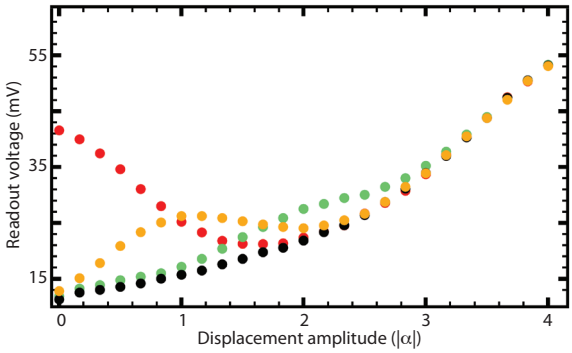

Figure 2: **Cross Kerr readout voltage subtraction. a**, Readout voltage for the selective pulses X_π^n applied to $n = 0, 1, 4$ (•, •, •) for a 10 ns displacement with amplitude $|\alpha|$ of the cavity ground state. • is the control experiment without applying a photon number selective pulse. This shows, that due to the Cross-Kerr we get higher and higher readout voltages for more average photons in the cavity without exciting the qubit. Subtracting the background experiment from the measured Fock state probabilities leads to the data shown in Fig.3b.

6 Cavity displacement & displacement calibration

The cavity is displaced using a 10 ns pulse resonant with the $|0\rangle \rightarrow |1\rangle$ transition of the cavity creating a photon number probability distribution given by a coherent state. We can measure the probability of finding the Fock state $|n\rangle$ by applying a photon number state selective π pulse to the qubit and measure the qubit excitation. The displacement voltage ϵ applied to the cavity is calibrated in units of the average photon number in the cavity $\bar{n}$, or rather the corresponding displacement amplitude $|\alpha| = \sqrt{\bar{n}}$, by fitting a Poisson distribution $P_n(\epsilon) = (\frac{\epsilon}{\Delta\epsilon})^{2n} e^{(\epsilon/\Delta\epsilon)^2}/n!$, with the normalization constant $\Delta\epsilon$, to all measured photon number probabilities simultaneously. The probability of finding the Fock states $n = 0 \ldots 7$ for a displacement with amplitude $|\alpha|$ of the ground state can be seen in Fig.3b. The probabilities closely follow the expected Poisson distribution. This demonstrates that it is possible to create a coherent state despite the cavity non-linearity as long as the displacement pulse has a large enough spectral width.

7 Excited state qubit population and negative values in the Hussimi Q-function.

We found, that the qubit has a 10% excited state population p_e which has been observed in other 3D superconducting qubits [6, 7] but is not yet completely understood. In our case this excited state qubit population leads to negative values in the Hussimi Q-function, as can be seen in Fig. 3a of the main text. These negative values are a result of the measurement procedure described in section 4. At the start of the experiment we create the combined qubit cavity state

$$\rho = (p_g |g\rangle \langle g| + p_e |e\rangle \langle e|) \otimes |\beta\rangle \langle \beta| . \tag{8}$$

With $p_g(p_e)$ the probability of finding the qubit in the ground(excited) state. The resonator state for the qubit in the excited state evolves at a rate different by χ compared to the ground state qubit resonator

$$\rho = p_g |g\rangle \langle g| \otimes |\beta\rangle \langle \beta| + p_e |e\rangle \langle e| \otimes \left|e^{i\chi t}\beta\right\rangle \left\langle e^{i\chi t}\beta\right| . \tag{9}$$

Here we completely neglect the evolution due to the Kerr effect as it happens on much slower timescales.For an analysis displacement $D(\alpha)$ that brings neither of the coherent states back to the ground state but e.g. displaces them even further we get the state

$$\rho = p_g |g\rangle \langle g| \otimes |\beta_1\rangle \langle \beta_1| + p_e |e\rangle \langle e| \otimes |\beta_2\rangle \langle \beta_2| \tag{10}$$

with $|\beta_1\rangle = D(\alpha)|\beta\rangle$ and $|\beta_2\rangle = D(\alpha)\left|e^{i\chi t}\beta\right\rangle$. Applying a state selective pi pulse X_π^0 does not change the state such that this experiment and the control experiment omitting the π pulse will result in the same readout Voltage. This means that $Q_0(\alpha) = 0$ still corresponds to 0 readout voltage in the presence of inital excited state qubit population.

For an analysis displacement that brings the state $\left|e^{i\chi t}\beta\right\rangle$ to the ground state $|0\rangle$, followed by a state selective pi pulse X_π^0, we will flip the excited state qubit to the ground state while leaving the ground state qubit untouched and displacing $|\beta\rangle$ to a new $|\beta'\rangle$

$$\rho = |g\rangle \langle g| \otimes (p_g |\beta'\rangle \langle \beta'| + p_e |0\rangle \langle 0|). \tag{11}$$

When we now subtract the control experiment we find a readout voltage which is negative

$$V_{neg} = -p_e(V_{e,0} - V_{g,0}) < 0 \tag{12}$$

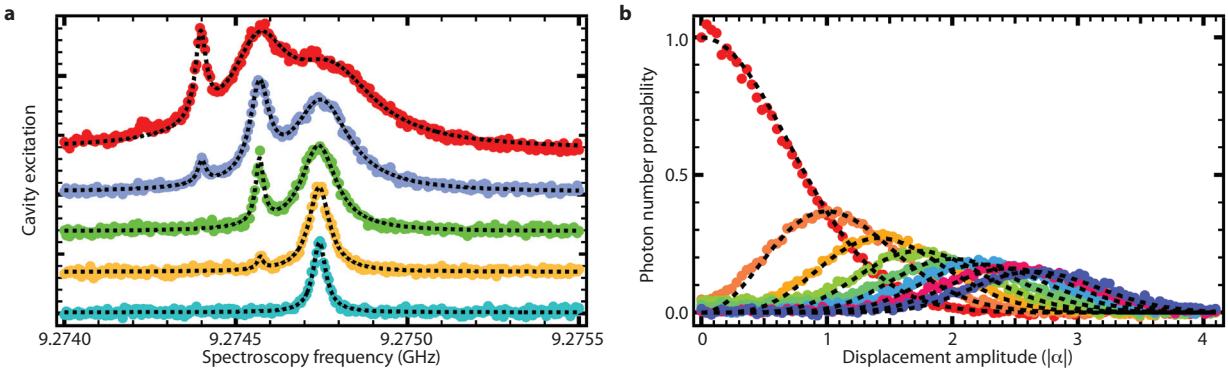

Figure 3: **Cavity spectroscopy for varying spectroscopy power and displacement calibration. a**, The cavity excitation is measured by mapping the population left in the ground state to the qubit using a photon number state selective π pulse. For the lowest power (•) the cavity is only excited on the $|0\rangle \rightarrow |1\rangle$ transition. As the power is increased (• $\rightarrow$ • $\rightarrow$ • $\rightarrow$ • $\rightarrow$ •) different transitions appear in the spectroscopy. These transitions are n-photon transition from $|0\rangle$ to $|n\rangle$ with $n = 1, 2, 3$ labeled from the right peak to left. The separation between the peaks is given by $0.5\,K/2\pi = 163$ kHz. The dashed lines are fit to the data using a multipeak Lorentzian function. **b**, Photon number probability of the Fock states $n = 0 \ldots 7$ (•, •, •, •, •, •, •, •) for a 10 ns displacement with amplitude $|\alpha|$ of the cavity ground state. The axes were scaled by fitting a Poisson distribution with two free fit parameters to all seven Fock state populations simultaneously. The dashed lines are given by a Poisson distribution $P(|\alpha|) = |\alpha|^{2n} e^{-|\alpha|^2}/n!$ for the Fock state n.

thus leading to negative values in the Q_0 measurements. Effectively we are measuring Q_0 for the qubit in the ground state, minus Q_0 for the qubit in the excited state which exactly corresponds to Q_0 of the resonator if the qubit is perfectly cold.

Furthermore, the evolution of the coherent state correlated with an excited state qubit will also generate q-component cat states which have negative readout voltages. This will reduce the amplitudes and coherent fringes of the observed cat states as the amplitudes of our Q_n measurements are scaled to the amplitude of the coherent state of Fig. 3a in the main text. Effectively, the excited state population will lead to a reduction of the fidelity for the measured cat states.

8 Cavity state tomography

Using the photon number state selective pulse to project onto the n$^{\text{th}}$ photon Fock state, along with a preceding cavity displacement, we can measure (see Fig. 4):

$$Q_n(\alpha_m) = \frac{1}{\pi}\langle n|D(-\beta_m)\rho D(\beta_m)|n\rangle \tag{13}$$

where n is the fock state projection; β_m,the tomography displacement; and ρ, the cavity density matrix. The Q_n are normalized probability distributions. Assuming a truncated photon basis, we are also able to directly reconstruct the cavity Wigner function [8, 9]:

$$\begin{aligned} W(\alpha_m) &= \frac{2}{\pi}\,\mathrm{Tr}(D(-\alpha_m)\rho D(\alpha_m)P) \\ &= \frac{2}{\pi}\sum_n (-1)^n \langle n|D(-\alpha_m)\rho D(\alpha_m)|n\rangle \\ &= 2\sum_n (-1)^n Q_n(\alpha_m) \end{aligned} \tag{14}$$

where P is the photon number parity operator. A more effective method for determining the Wigner function of the resonator is to reconstruct its density matrix. Realizing that the Q_n are a set of linear equations, we can rewrite Eqn. 13 as:

$$Q_n(\alpha_m) = \frac{1}{\pi}\sum_{ij} M_{nmij}\rho_{ij} \tag{15}$$

where $M_{nmij} = \langle n|D(-\alpha_m)|i\rangle\langle j|D(\alpha_m)|n\rangle$ and $\rho_{ij} = \langle i|\,\rho\,|j\rangle$. Measuring the distributions, $Q_n(\alpha_m)$, with known photon projections n and displacements α_m, we can perform a least squares regression to determine the cavity state, ρ. For this experiment, we measured 441 displacements each for projections onto the Fock states with 0 to 7 photons, 3528 measurements in total with 1000 averages per measurement point for each regression. We perform the linear

regression with a priori assumptions that the cavity density matrix is Hermitian, of trace one, positive semi-definite and having a trunctated basis of ten photons. This reconstructed density matrix is then used to calculate state fidelities and plot Wigner functions (see Fig. 5).

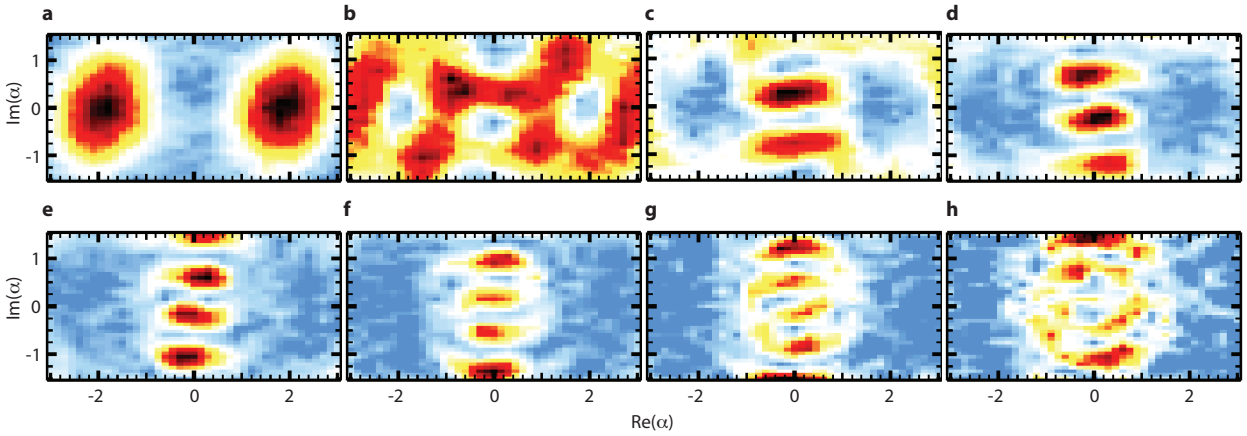

Figure 4: $\boldsymbol{Q_n(\alpha)}$ **probability distributions. a-h**, show the measured projections on the Fock states with $n = 0 - 7$ for the two-component Schrödinger cat state shown in Fig.5a . Each $Q_n(\alpha)$ was measured at 441 different displacements α. The different $Q_n(\alpha)$ functions were measured by conditioning the qubit π pulse on the photon number in the cavity.

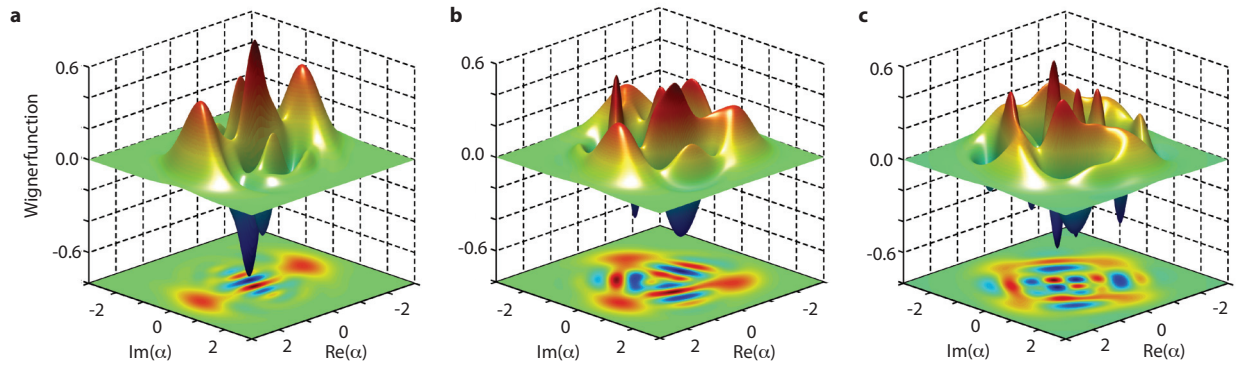

Figure 5: **Wigner function plot of the multi-component cat states emerging during the Kerr interaction.** The frames are measured after an evolution of **a** 1540 ns, **b** 1010 ns, and **c** 760 ns. The Wigner functions are reconstructed using a least mean square fit on the measurements of $Q_n(\alpha)$ for $n = 0 - 7$.

References

[1] Nigg, S. E. *et al.* Black-box superconducting circuit quantization. *Physical Review Letters* **108**, 240502 (2012).

[2] Johnson, B. R. *et al.* Quantum non-demolition detection of single microwave photons in a circuit. *Nature Physics* **6**, 663–667 (2010).

[3] Solano, E. Selective interactions in trapped ions: State reconstruction and quantum logic. *Physical Review A* **71**, 013813 (2005).

[4] França Santos, M., Solano, E. & de Matos Filho, R. Conditional Large Fock State Preparation and Field State Reconstruction in Cavity QED. *Physical Review Letters* **87**, 093601 (2001).

[5] Reed, M. *et al.* High-Fidelity Readout in Circuit Quantum Electrodynamics Using the Jaynes-Cummings Nonlinearity. *Physical Review Letters* **105**, 173601 (2010).

[6] Córcoles, A. D. *et al.* Protecting superconducting qubits from radiation. *Applied Physics Letters* **99**, 181906–181906–3 (2011).

[7] Sears, A. P. *et al.* Photon Shot Noise Dephasing in the Strong-Dispersive Limit of Circuit QED. *arXiv.org* **1206.1265** (2012).

[8] Hofheinz, M. *et al.* Synthesizing arbitrary quantum states in a superconducting resonator. *Nature* **459**, 546–549 (2009).

[9] Leibfried, D. *et al.* Experimental determination of the motional quantum state of a trapped atom. *Physical Review Letters* **77**, 4281–4285 (1996).